This article was downloaded by:
On: *25 January 2011*
Access details: *Access Details: Free Access*
Publisher *Taylor & Francis*
Informa Ltd Registered in England and Wales Registered Number: 1072954 Registered office: Mortimer House, 37-41 Mortimer Street, London W1T 3JH, UK


**Liquid Crystals**
Publication details, including instructions for authors and subscription information:
http://www.informaworld.com/smpp/title~content=t713926090

# Response mechanism of a vertical alignment mode driven by fringe-field switching

Hongmei Ma[a]; Yubao Sun[abc]; Guangsheng Fu[b]
[a] Department of Applied Physics, Hebei University of Technology, Tianjin, People's Republic of China [b] School of Information Engineering, Hebei University of Technology, Tianjin, People's Republic of China [c] Center for Display Research, Department of Electronic and Computer Engineering, University of Science and Technology, Clear Water Bay, Kowloon, Hong Kong

**To cite this Article** Ma, Hongmei , Sun, Yubao and Fu, Guangsheng(2009) 'Response mechanism of a vertical alignment mode driven by fringe-field switching', Liquid Crystals, 36: 9, 999 — 1002
**To link to this Article: DOI:** 10.1080/02678290903215345
**URL:** http://dx.doi.org/10.1080/02678290903215345

PLEASE SCROLL DOWN FOR ARTICLE

Full terms and conditions of use: http://www.informaworld.com/terms-and-conditions-of-access.pdf

This article may be used for research, teaching and private study purposes. Any substantial or systematic reproduction, re-distribution, re-selling, loan or sub-licensing, systematic supply or distribution in any form to anyone is expressly forbidden.

The publisher does not give any warranty express or implied or make any representation that the contents will be complete or accurate or up to date. The accuracy of any instructions, formulae and drug doses should be independently verified with primary sources. The publisher shall not be liable for any loss, actions, claims, proceedings, demand or costs or damages whatsoever or howsoever caused arising directly or indirectly in connection with or arising out of the use of this material.

*Liquid Crystals,*
Vol. 36, No. 9, September 2009, 999–1002

Taylor & Francis
Taylor & Francis Group

# Response mechanism of a vertical alignment mode driven by fringe-field switching

Hongmei Ma[a], Yubao Sun[a–c]* and Guangsheng Fu[b]

[a]*Department of Applied Physics, Hebei University of Technology, Tianjin 300401, People's Republic of China;* [b]*School of Information Engineering, Hebei University of Technology, Tianjin 300401, People's Republic of China;* [c]*Center for Display Research, Department of Electronic and Computer Engineering, Hong Kong University of Science and Technology, Clear Water Bay, Kowloon, Hong Kong*

*(Received 27 May 2009; final form 27 July 2009)*

The response mechanism of a vertical alignment mode, driven by a fringe field, is investigated in detail using small-angle approximation. The flow effects can be ignored when using theoretical analysis. The period of the liquid crystal (LC) deformation in the transversal direction, instead of the lognitudinal direction, shows the cell gap effect on the response time in the LC layer's thickness. The authors' analytical results indicate that a liquid crystal display (LCD) mode with a small transversal period could provide a new method that gives a fast response.

**Keywords:** response mechanism; vertical alignment; fringe field switching

Downloaded At: 14:30 25 January 2011

## 1. Introduction

During the past 20 years, liquid crystal display (LCD) modes with a fast response and a wide viewing angle have been the topical research issue in the application of LCDs (*1*) and many nematic LCD modes have been proposed. In-plane switching (IPS) (*2*) and fringe-field switching (FFS) (*3*) modes have a wide viewing angle, but their response is slow for twist deformation. Several vertical alignment (VA) modes, such as multi-domain VA (*4*), patterned VA (*5*) and advanced super-V (*6*), show fast responses because of their bend deformation (*7*). The optically compensated bend (OCB, or Pi cell) mode has the advantage of a very fast response speed, but has a relatively narrow viewing angle compared with that of the other modes listed above (*8*).

Several techniques are used to improve the response speed, such as having a thinner cell gap, using the overdrive and undershoot method, using low-viscosity liquid crystal (LC) materials and operating in elevated temperatures (*1*). Among them, reducing the cell gap is considered conventionally as the major method for obtaining a faster response because the response time is proportional to the cell gap's square. However, a thick cell, vertically aligned and driven by dual FFS (FFS-VA) mode, was proposed and takes the advantages of both the fast response and wide viewing angle (*9*). In this mode, the thickness of the LC layer is more than 10 μm, which is larger than the conventional thickness, but its response time can be reduced to less than 1 ms, which can be used in any type of LCD application. The response times for this mode are more than 16 times faster than that of normal VA mode LCDs, but the fast response mechanism has not been clear up to until now and it cannot be explained obviously by the conventional theory.

In this paper, we investigate the response mechanism of this thick cell FFS-VA mode. Our theoretical analysis shows that the backflow and flow effect of LCs can be ignored. The potential distribution and the LC deformation are periodic in the transversal direction. The transversal period of the LC director's deformation, instead of the lognitudinal LC layer thickness, shows the cell gap's effect on the response time. The theoretical results are also confirmed by the numerical simulation.

## 2. Model and theory

In the thick cell with dual FFS electrodes, the electric field near the substrate is much stronger than that in the middle of the LC cell, as shown in Figure 1(a). ZLI-4792 LC material with positive dielectric anisotropy ($\Delta\varepsilon > 0$) is used in a numerical simulation with a two-dimensional LC simulator (LCD Master developed by Shintech). The LC is perpendicular to the substrate at the initial state, moving in the electric field after the driven voltage is added. The width ($W$) and gap ($G$) of the pixel electrodes inside the common electrodes is equal to 2 μm (*9*). The driven voltage is 10 V, the surface anchoring is $5 \times 10^{-4}$ J m$^{-2}$, and the cell gap is 10 μm. From Figure 1(a), we see that the LCs far from the substrates do not tilt, that is to say, the bottom and top electrodes have no effect on each other. Moreover, the LC molecules above the centre of

*Corresponding author. Email: hmtj450@vip.sina.com

ISSN 0267-8292 print/ISSN 1366-5855 online
© 2009 Taylor & Francis
DOI: 10.1080/02678290903215345
http://www.informaworld.com

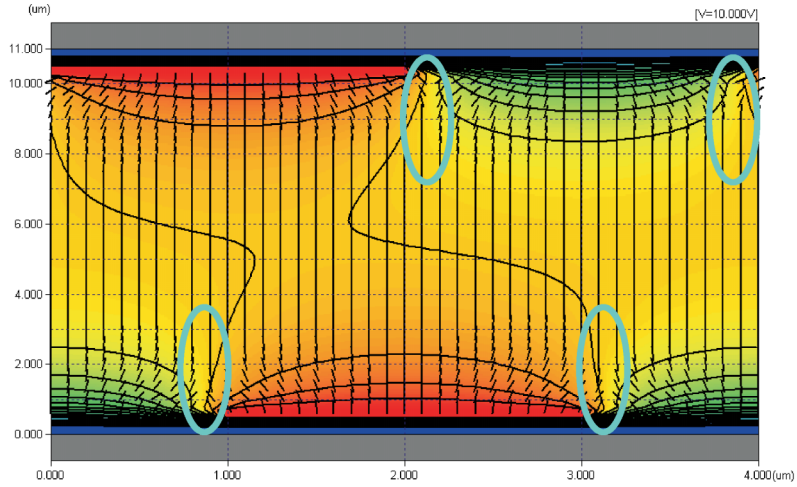


(a)

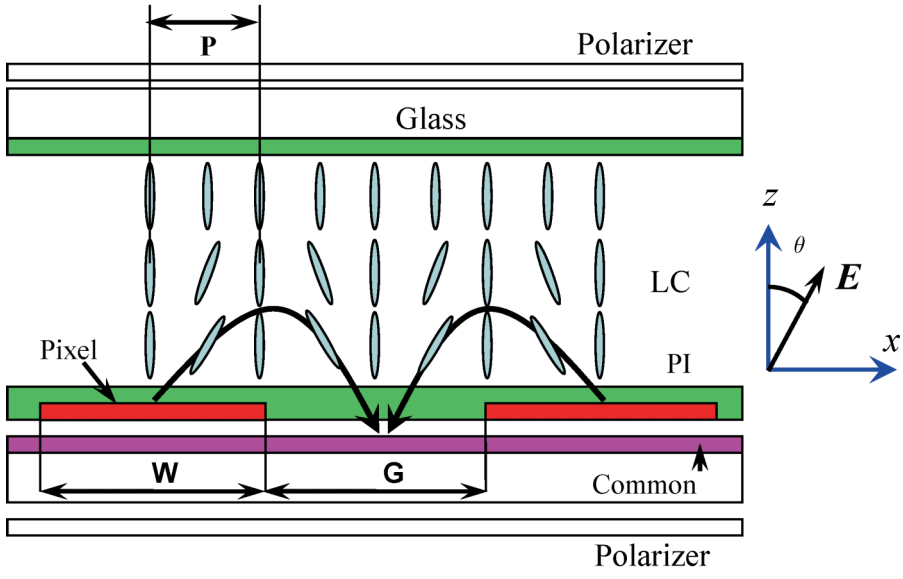


(b)

Figure 1. (a) The potential and LC distributions of the thick cell dual FFS-VA mode driven by 10 V. (b) Device structure of the FFS-VA mode in theoretical analysis.

the electrodes and the gap also do not tilt because of the weak transverse electric field. In the ellipses near the edges of the pixel electrodes, the LCs tilt down oppositely and there is no downwards tilt in the LCs a slightly further away from substrates. In this case, we can assume that some LCs in these ellipses cannot tilt, even though there is a strong transversal electric field. Therefore, we can use the ideal structure model as illustrated in Figure 1(b) to analyse the response mechanism of the thick cell DFFS-VA mode. The LC molecules without tilt deformation appear at the edges and the centre of the pixel electrodes and the centre of the gaps of the pixel electrodes. The periods of the electric field and the LC deformation are $P_E = (W + G)/2$ (for the electric field) and $P_d = (W + G)/4$ (for the LC deformation).

In the LC layer, the electric field distribution induced by the FFS electrodes has been investigated as the comb-on-plane switching mode (*10*). The horizontal and vertical components of the electric field for $W = G$ are

Downloaded At: 14:30 25 January 2011

$$E_x = -\frac{V}{P_d}\sin\frac{x\pi}{2P_d}\cosh\frac{z\pi}{2P_d}\Big/\left(\cos\frac{x\pi}{P_d}+\cosh\frac{z\pi}{P_d}\right), \tag{1a}$$

$$E_z = -\frac{V}{P_d}\cos\frac{x\pi}{2P_d}\cosh\frac{z\pi}{2P_d}\Big/\left(\cos\frac{x\pi}{P_d}+\cosh\frac{z\pi}{P_d}\right). \tag{1b}$$

Here, $V$ is the voltage applied to the pixel electrodes and $x = 0$ and $z = 0$ correspond to the centre of the electric gap and the bottom substrate surface, respectively. In the LC layer, the $x$-component of the electric field has a period ($P_E = 2P_d$) and drives LC molecules to the electric field direction, but the $z$-component holds the vertical alignment. In a different spatial position, the angle of the LC director and the electric field direction is

$$\theta(x) = \tan^{-1}\left(\frac{Ex}{Ez}\right) = \frac{x\pi}{2P_d}. \tag{2}$$

Here, $\theta(x)$ is linearly dependent on $x$, but independent of $z$. In our earlier paper (*11*), we analysed the response mechanism of the OCB cell. In an OCB cell, the electric field is perpendicular to the substrate surface and the LCs' tilt angles vary with $z$. Comparing the relationship of the LC director and the electric field direction, we can see that the LC deformation in the $x$-axis of this mode is similar to that in the $z$-axis of OCB mode.

Now, we reconstruct the LC cell along the $x$-axis. In the reconstructed LC cell (illustrated in Figure 2), in which the cell gap is $P_E = 2P_d$, the LCs are parallel to the surface, and the arrows represent the electric field directions and the length means the strength of the electric field. The LC at the surface does not change its angle because the electric field direction is parallel to the LC direction. The LC in the middle layer also does not change because the forces induced by the upper and lower LC deformations cancel each other. In the OCB cell, the backflow effect can be ignored because of the same flow direction in the upper and lower parts of LC layer, but flow effect must be considered because there is no period wall to cancel the flow. In this reconstructed cell, the backflow effect can be ignored because of the opposite tilt change in the upper and lower parts and because there is no change in the middle layer. The flow directions in the two parts are the same and along the $z$-axis, and the flow effects can be cancelled by the real substrate surfaces. Moreover, the flows of the two parts in the $x$-axis are opposite and equal to each other, which implies that the flow effect can be ignored. Then, we have the dynamic equation without the flow effect for this mode (*11–13*):

$$\gamma\frac{d\phi}{dt} = \left(K_{11}\sin^2\phi + K_{33}\cos^2\phi\right)\frac{\partial^2\phi}{\partial x^2} + \left[(K_{33}-K_{11})\left(\frac{d\phi}{dx}\right)^2 + \varepsilon_0\Delta\varepsilon E^2\right]\sin\phi\cos\phi, \tag{3}$$

where $K_{11}$ and $K_{33}$ are the splay and bend elastic constant, respectively, $\Delta\varepsilon$ is the dielectric anisotropy, $\phi$ is the changed angle of the LC tilt angle, which changes with time ($t$) and position ($x$) and $\gamma$ is the bulk rotational viscosity. Using small-angle approximation, the LC profile for the decay processes can be written as (*11*, *14*, *15*)

$$\varphi_{\text{decay}}(z,t) = \varphi_m \sin\frac{2\pi x}{P_E}\exp(-t/\tau_d). \tag{4}$$

Here, $\phi_m$ is the maximum deformation of the LC under an electric field. To obtain the decay times, we can use one elastic constant approximation ($K_{11} = K_{33}$) and let $t = \tau$. Substituting Equation (4) into Equation (3), we get the decay time for the cell switched from the on state to the off state:

$$\tau_d = \frac{\gamma P_E^2}{4\pi^2 K_{33}}. \tag{5}$$

With the decay time ($\tau_0 = \gamma d^2/(\pi^2 K_{33})$) of the conventional VA cell (*15*), the decay time of the FFS-VA mode becomes

$$\tau_d = \frac{1}{4}\left(\frac{P_E}{d}\right)^2\tau_0, \tag{6}$$

which shows that the response speed of FFS-VA cell is four times faster than that of the conventional VA

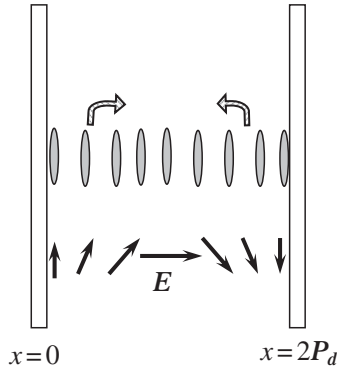


Figure 2. The reconstructed LC cell in the $x$-axis and the electric field distribution.

Downloaded At: 14:30 25 January 2011

Table 1. Comparison of the theoretical and numerical optical decay times.

| | Cell I (*9*) | Cell II (*9*) | T part (*16*) | R part (*16*) |
|---|---|---|---|---|
| Theoretical results | 1.08 ms | 0.33 ms | 2.06 ms | 0.81 ms |
| Numerical results | 1.05 ms[a] | 0.37 ms[a] | 2.1 ms[b] | 0.9 ms[b] |

Notes: [a]From 1/8 grey level to dark. [b]From 1/2 grey level to dark.

cell, even if $P_E = d$. In fact, the cell gap of the conventional VA cell is usually above 4 μm, and $P_E$ is in the range 2–5 μm in the FFS mode because the width and gap of electrodes are around 2–5 μm (see (*9*)). As a result, the improvement of the response time depends on the period of the LCs' deformation or the electric field; the response is improved more than 16 times if $P_E$ is less than 2 μm using the FFS-VA mode. For the rise time, the improvement is the same as the decay time, because the rise time is proportional to the decay time with a factor that includes the driven electric field (*15*).

The response time of the LC director in the $z$-axis is the same to that in the $x$-axis, and the response time of the optical transmission has a direct relation with the LC's response time in the $x$-axis. Dr Wang gives the ratio of the optical decay time and the LC director decay time as about 0.62, derived from the numerical calculation when the driven voltage is a little larger than the threshold voltage (*15*). Now, we examine the optical decay time in the thick cell dual FFS-VA mode (*9*, *16*) using our results. Substituting the parameters of the LC and the pixel electrodes in Equation (5) and the ratio (0.62), the calculated optical decay times compared with the numerical optical decay times (simulated by TechWiz 3D developed by Sanayi) are shown in Table 1. We can see that the theoretical analysis is well confirmed by the numerical results.

## 3. Conclusion

In summary, the response mechanism of the FFS-VA cell was investigated. The backflow and flow effects are neglected because of the opposite tilt change. The period of the LC deformation in the transversal direction, instead of the thickness of the LC layer in the lognitudinal direction, shows the cell gap effect in the critical formula of the response times. The thin period of the LC deformation shows an improvement of more than sixteen times. The shortcoming of this thick cell DFFS-VA mode with the positive LC material is the rigorous contraposition of the top and bottom pixel electrodes, which can be very difficult. This mode, with negative dielectric anisotropic LC material, should solve this problem (*17*). The theoretical results have a potential application in designing fast-response LCDs in the future.

## Acknowledgements

The authors would like to thank Dr M. Jiao and Professor S. T. Wu of the University of Central Florida for their technical discussion. This research was supported by the Key Subject Construction Project of Hebei Province University and the National Natural Science Foundation of China (No.10704022 and 60736042), P. R. China.

## References

(1) Yang, D.K.; Wu, S.T. *Fundamentals of Liquid Crystal Devices*; John Wiley and & Sons Ltd., Chichester, 2006.
(2) Oh-e, M.; Kondo, K. *Appl. Phys. Lett.* **1995**, *67*, 3895–3897.
(3) Lee, S.H.; Lee, S.L.; Kim, H.Y. *Appl. Phys. Lett.* **1998**, *73*, 2881–2883.
(4) Ohmuro, K.; Kataoka, S.; Sasaki, T.; Koike, Y. *SID Int. Symp. Digest Tech. Papers* **1997**, *28*, 845–848.
(5) Kim, K.H.; Lee, K.H.; Park, S.B.; Song, J.K.; Kim, S.N.; Souk, J.H. In Proceedings 18th International Display Research Conference (Asia Display' 98), Seoul, Korea, 1998; pp. 383–386.
(6) Pollack, J. *Inf. Disp.* **1999**, *15*, 16.
(7) Lyu, J.J.; Sohn, J.; Kim, H.Y.; Lee, S.H. *J. Disp. Tech.* **2007**, *3*, 404–412.
(8) Yamaguchi, Y.; Miyashita, T.; Uchida, T. *SID Int. Symp. Digest Tech. Papers* **1993**, *24*, 277.
(9) Jiao, M.; Ge, Z.; Wu, S.T.; Choi, W.K. *Appl. Phys. Lett.* **2008**, *92*, 111101.
(10) Meng, Z.; Kwok, H.S.; Wong, M. *J. Soc. Inf. Disp*. **2000**, *8*, 139.
(11) Sun, Y.; Ma, H.; Zhang, Z.; Fu, G. *Appl. Phys. Lett.* **2008**, *92*, 111117.
(12) Acosta, E.J.; Towler, M.J.; Walton, H.G. *Liq. Cryst.* **2000**, *27*, 977–984.
(13) Acosta, E.J.; Towler, M.J.; Tilin, M.D. *J. Appl. Phys.* **2005**, *97*, 093106.
(14) Sun, Y.; Zhang, Z.; Ma, H.; Zhu, X.; Wu, S.T. *Appl. Phys. Lett.* **2002**, *81*, 4907–4909.
(15) Wang, H.; Wu, T.X.; Zhu, X.; Wu, S.T. *J. Appl. Phys.* **2004**, *95*, 5502–5508.
(16) Jiao, M.; Wu, S.T.; Choi, W.K. *J. Disp. Tech.* **2009**, *5*, 83–85.
(17) Sun, Y.; Kwok, H.S. *ASID*. **2009**, in press

Downloaded At: 14:30 25 January 2011